Original Article | Thorax

eISSN 2005-8330
https://doi.org/10.3348/kjr.2024.0818
Korean J Radiol 2025;26(5):498-507

Korean Journal of Radiology
KJR

Feasibility of Multiparameter MRI-Guided Percutaneous Biopsy for Central Lung Lesions With Atelectasis

Peipei Li[1]*, Chengli Li[2]*, Yujun Xu[2], Xiangmeng He[2], Roberto Blanco Sequeiros[3], Ming Liu[2]

[1]Department of Oncology, Shandong Rehabilitation Research Center Shandong Rehabilitation Hospital, Jinan, China
[2]Department of Interventional MRI, Shandong Provincial Hospital Affiliated to Shandong First Medical University, Jinan, China
[3]The South Western Finland Imaging Centre, Turku University Hospital, Turku, Finland

Objective: To prospectively evaluate the feasibility, accuracy, and safety of multiparameter MRI-guided percutaneous biopsy using a 1T open MRI scanner for evaluating suspicious centrally located lung lesions with associated post-obstructive atelectasis.

Materials and Methods: In this single-center study, MRI-guided percutaneous coaxial cutting biopsy was performed for 107 suspicious central lung lesions with associated post-obstructive atelectasis in 107 patients between July 2015 and December 2020. A fast T2-weighted imaging (T2WI)-turbo spin echo (TSE) sequence and an enhanced fast T1-weighted imaging (T1WI)-TSE sequence were used to identify, localize, and biopsy lung lesions, and diffusion-weighted imaging (DWI) was used as a supplementary sequence for identifying the lesion location. The final diagnosis was confirmed by surgical histopathology or clinical follow-up for a minimum of 24 months. The sensitivity, specificity, and accuracy for diagnosing lung malignancies were calculated, and the complications were recorded for each case.

Results: Using multiparameter MRI, central lung lesions could be clearly distinguished from post-obstructive atelectasis in 96 patients (89.7%). The sensitivity, specificity, and accuracy of MRI-guided percutaneous biopsy for diagnosing lung malignancy was 97.0% (98/101), 100% (6/6), and 97.2% (104/107), respectively. Self-limited hemoptysis occurred in three patients. Pneumothorax occurred in five patients, of which none required pleural drainage. No serious procedure-related complications were observed.

Conclusion: As a technology that does not involve ionizing radiation, multiparameter MRI-guided percutaneous coaxial cutting biopsy is a safe and accurate diagnostic technique for evaluating centrally located lung lesions associated with post-obstructive atelectasis.

Keywords: Magnetic resonance imaging; Interventional radiology; Lung neoplasms; Biopsy; Technology

INTRODUCTION

Central lung cancer is usually located near the lung hilum, making surgical resection difficult. In such cases, obtaining a definitive pathological diagnosis and molecular profiling of the tumor are of utmost importance if radiotherapy, chemotherapy, biological targeted therapy, or immunotherapy are planned. Centrally located lung cancer often causes obstructive pneumonia, resulting in lung volume loss and subsequent atelectasis [1,2]. Thus, distinguishing lung cancer from atelectasis is extremely important for determining the extent of the local tumor and targeting lesions for biopsy. Bronchoscopy is the most common method used for pathological diagnosis of central pulmonary lesions, and its sensitivity for detecting malignancies ranges from 82% to 94% [3-7]. However, the presence of atelectasis can influence the diagnostic accuracy of bronchoscopy for central lung cancer, even when endobronchial ultrasound-transbronchial needle aspiration (EBUS-TBNA) is used [3,8]. Occasionally, primary lung lesions are associated with parenchymal consolidation with

Received: August 21, 2024 **Revised:** February 18, 2025
Accepted: February 20, 2025
*These authors contributed equally to this work.
Corresponding author: Ming Liu, MD, Department of Interventional MRI, Shandong Provincial Hospital Affiliated to Shandong First Medical University, Jingwu Road 324, Jinan, Shandong 250021, China
• E-mail: mingliu800124@163.com

Korean Journal of Radiology
KJR

Table 1. The inclusion and exclusion criteria for this study

Inclusion criteria	Exclusion criteria
1. The lung lesion initially detected without undergoing anti-tumor treatment	1. Severe emphysema and bullae preventing safe approach by biopsy
2. A requirement for biopsy to obtain definitive pathological diagnosis and/or molecular profiling necessary for the further treatment plan	2. Serious coagulation disorders (international normalized ratio of more than 1.5 or an activated partial thromboplastin time of more than twice the normal value)
3. A presumed intrapulmonary mass with the medial margin located within the inner third of the hemithorax on CT	3. Platelet disorders (fewer than 50 x 10^9/L)
4. Suspicious malignant central lung lesions with atelectasis on CT	4. Contraindications to MRI (cardiac pacemaker, etc.)
5. The presumed lesion diameter ≥1.5 cm on CT	5. Patients who were not able to cooperate during the procedure (frequent cough or poor physique)

inflammatory or fibrotic reactions around the main tumor, rendering the tumor undistinguishable on ultrasound [3].

CT is the most widely used imaging method for patients with thoracic diseases. CT provides excellent spatial resolution; however, its inherently poor soft-tissue contrast limits its ability to distinguish some tumors from atelectasis, even with intravenous contrast [2]. PET-CT is excellent for detecting tumors within atelectasis, but its high radiation dose and cost limit its wide application [9,10]. In comparison with CT, MRI provides excellent soft-tissue contrast, direct multiplanar capabilities, multisequence imaging, and functional imaging [11-13]. The ability to distinguish tumors from atelectasis has remarkably improved [14]. In this study, we prospectively evaluated the feasibility, accuracy, and safety of MRI-guided percutaneous biopsy for suspicious centrally located lung lesions with associated post-obstructive atelectasis.

MATERIALS AND METHODS

Study Patients

The study plan was approved by the Institutional Review Board of Shandong Provincial Hospital (IRB No. SD NSFC 2015-277). Informed consent for both participation in the research study and undergoing the procedures was obtained from all patients, and the risks, benefits, and alternatives were explained to the patients in detail. The inclusion and exclusion criteria for this study are shown in Table 1, and the study flow diagram is presented in Figure 1. From July 2015 to December 2020, 113 patients were initially referred for MRI-guided biopsy on the basis of the inclusion criteria, and six patients were subsequently excluded on the basis of the exclusion criteria (severe emphysema, four cases; frequent cough, two cases). A total of 107 patients were enrolled in this study.

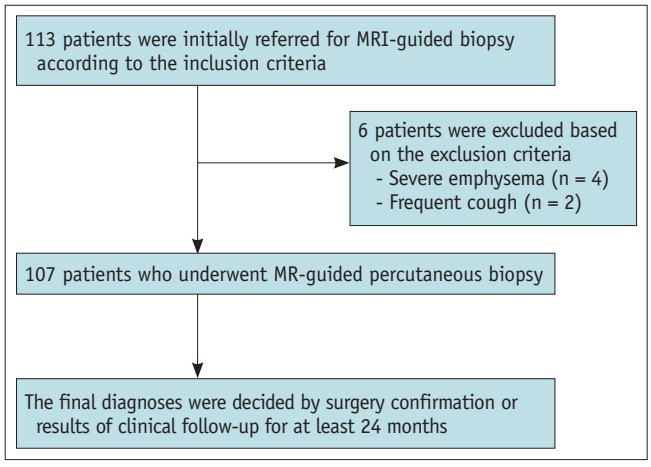

Fig. 1. Flow diagram for this study.

Equipment

We used a 1T open MRI scanner (Panorama HFO, Philips Healthcare, Best, The Netherlands) to guide percutaneous lung biopsy, a MR-compatible electrocardiogram monitor (MRGLIFE C Plus™, Schiller Medical, Bern, Switzerland) to continuously monitor vital signs during the procedure, and a 16-G or 18-G MR-compatible coaxial needle (Wanlin Medical, Qingdao, China) and a 18-G or 20-G semi-automated cutting needle (TSK TM, TSK Laboratory, Tochigi-shi, Japan) to obtain core specimens. The details of these equipment are reported elsewhere [15].

MRI-Guided Biopsy Procedure

All biopsies were performed by two experienced interventional radiologists with more than five years of experience in interventional MRI.

https://doi.org/10.3348/kjr.2024.0818

Pre-Procedural Preparation

Preoperative imaging data were reviewed to locate the lesions, assess vascularity, and design the puncture path. The principles employed for designing the puncture approach included avoiding visible bullae and lung fissures and passing through the atelectasis to avoid puncturing the aerated lung to decrease the probability of pneumothorax. Patients were placed in the supine or lateral decubitus position based on lesion accessibility and the safest path to the lesion. The MRI protocols used for lesion localization and atelectasis identification included axial with sagittal/coronal fast T2-weighted imaging (T2WI)-turbo spin echo (TSE) (repetition time [TR], 2702 ms; echo time [TE], 90 ms; flip angle, 90°; slice thickness/separation, 5 mm/1 mm; field of view, 400 mm x 303 mm; matrix, 248 x 153; number of signal averages [NSA], 2; and acquisition time, 39 seconds) and enhanced fast T1-weighted imaging [T1WI]-TSE (TR, 576 ms; TE, 10 ms; flip angle, 90°; slice thickness/separation, 5 mm/1 mm; field of view, 350 mm x 302 mm; matrix, 176 x 115; NSA, 2; and acquisition time, 40.3 seconds). Fast T2WI-TSE usually shows post-obstructive atelectasis as tissue with a higher signal intensity than the central tumor, while enhanced fast T1WI-TSE shows atelectasis as tissue with a higher signal intensity than the central tumor. If atelectasis identification was not possible using these two sequences, diffusion-weighted imaging (DWI) sequences (TR, 1624 ms; TE, 73 ms; flip angle, 90°; slice thickness/separation, 5 mm/1 mm; field of view, 375 x 306; matrix, 108 x 87; b, 600 s/mm^2; NSA, 2; and acquisition time, 2 minutes 54 seconds) were used for supplementary scans. The largest lesion diameter was measured on the transverse images. To minimize breathing artifacts,

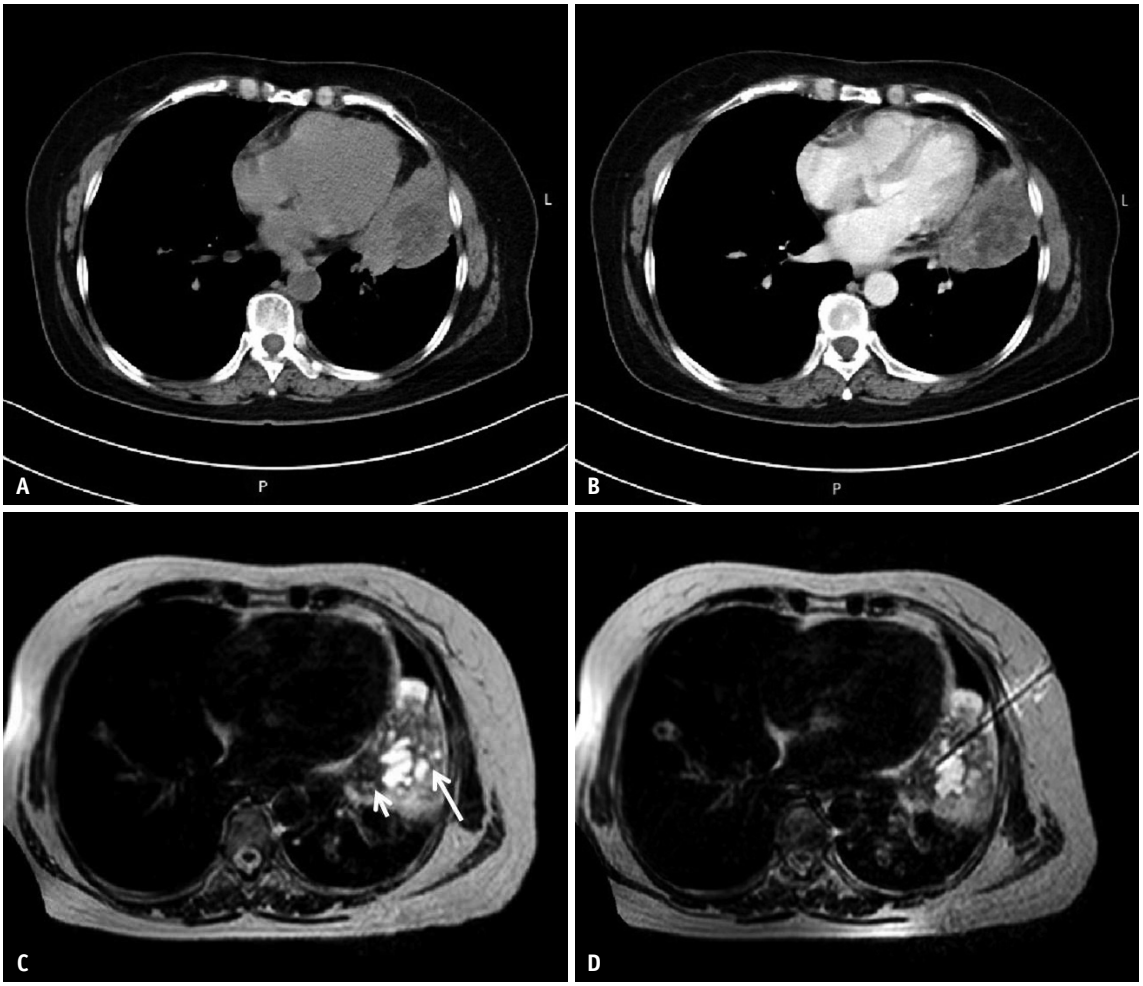

Fig. 2. A 61-year-old female with a lesion in the left upper lobe. **A, B:** Non-contrast-enhanced and contrast-enhanced CT did not allow reliable differentiation of tumors from the adjacent atelectasis. **C:** Fast T2-weighted imaging-turbo spin echo morphological MRI performed at the same level shows post-obstructive atelectasis (long arrow) with a higher signal intensity than the central tumor (short arrow), reflecting a higher water content. **D:** MRI-guided puncture needle in the lesion. The biopsy specimen revealed an adenocarcinoma.

https://doi.org/10.3348/kjr.2024.0818

Korean Journal of Radiology
KJR

especially in lower lung lesions, a respiratory gating system was employed during image acquisition. The needle entry point was determined by MRI using a matrix grid made of fish oil capsules, the details of which have been previously reported [15]. The approach angle, the distance from the skin to the parietal pleura, and the distance from the skin to the lesion were measured.

Biopsy Procedure

The selected entry site was prepared and draped in a sterile fashion, and local anesthesia (1% lidocaine) was administered subcutaneously. An MR-compatible coaxial needle was gradually inserted into the lesion. Two-cross-sectional images (axial with sagittal or coronal images) of fast T2WI-TSE or enhanced fast T1WI-TSE were acquired to determine the actual needle direction and position (Figs. 2-4). Once needle-tip placement within the target lesion was confirmed, the table was removed from the MRI scanner. The internal stylet was removed, and the samples were drawn using a semi-automated cutting needle. Three to seven core biopsies were performed for each lesion. If the puncture passed through the lung parenchyma, normal saline (3–10 mL) was instilled into the puncture access when the trocar needle was removed to seal the needle passage.

Post-Procedural Evaluation

Histological cores were fixed in 10% neutral buffered formalin for hematoxylin and eosin and immunohistochemical staining, if necessary. No rapid on-site cytopathological examinations were performed. The procedural time (the interval between the first acquisition and removal of the needle) was recorded. Immediately following biopsy, PD-weighted TSE with respiratory gating (TR, 1575 ms; TE, 30 ms; flip angle, 90°; slice thickness/

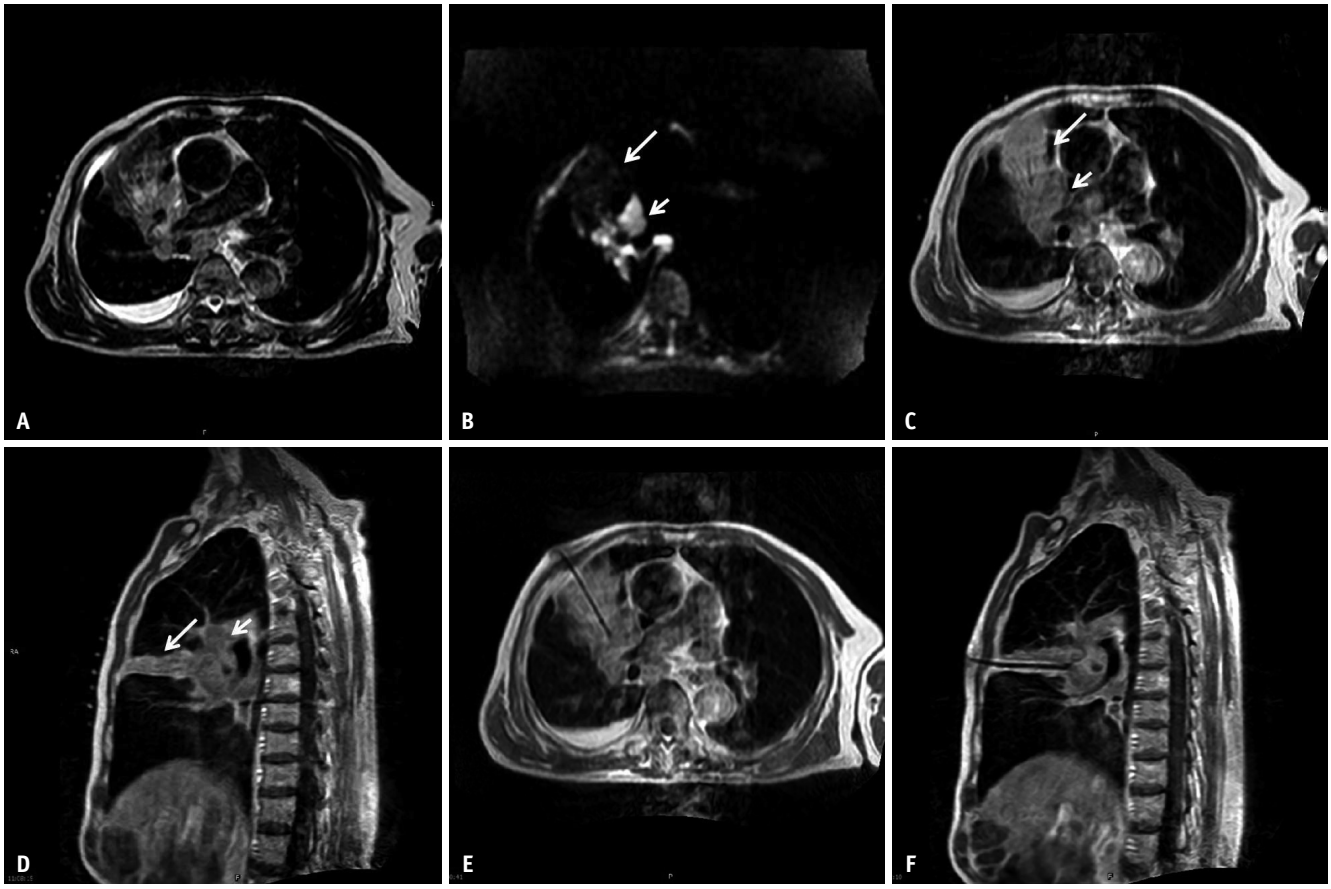

Fig. 3. A 72-year-old male with a lesion in the right upper lobe. **A:** Fast T2WI-TSE shows a lesion with heterogeneous signal intensity in the right upper lobe; however, the lesion cannot be easily distinguished from atelectasis. **B:** Diffusion-weighted imaging clearly depicts the difference in water restriction between the tumor tissue (short arrow) and the collapsed lobe (long arrow). **C, D:** Enhanced fast T1WI-TSE displays hyperintense atelectasis (long arrows) and hypointense lesions (short arrows) in transverse **(C)** and sagittal images **(D)**. **E, F:** Multiplanar MRI-guided puncture of the lesion. The biopsy specimen revealed small cell carcinoma. WI = weighted imaging, TSE = turbo spin echo

https://doi.org/10.3348/kjr.2024.0818

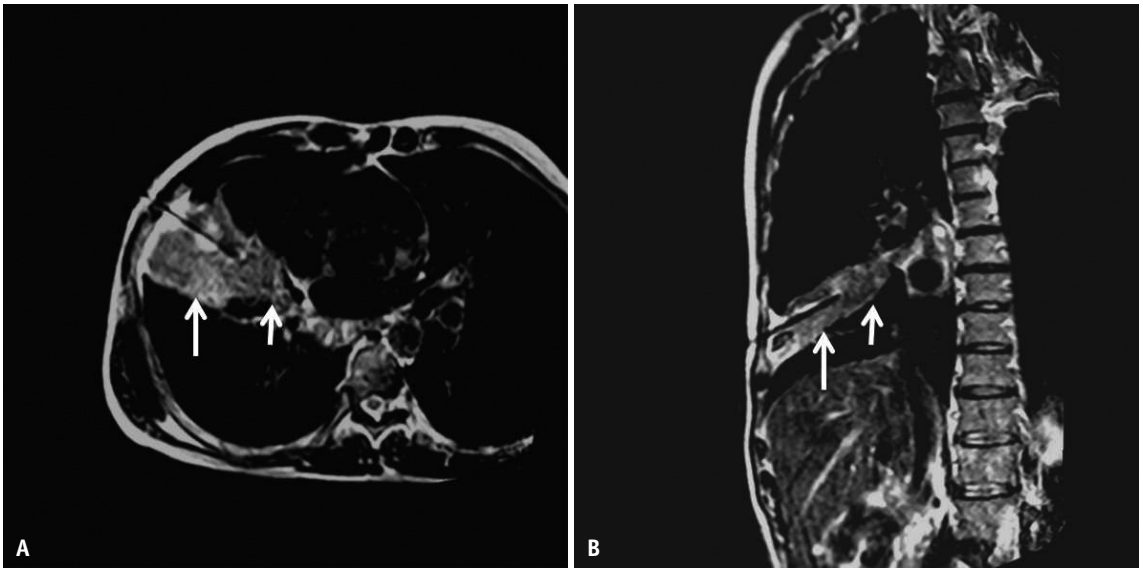

Fig. 4. A 54-year-old male with a lesion in the right middle lobe. **A, B:** Fast T2-weighted imaging-turbo spin echo transverse image **(A)** and coronal image **(B)** show post-obstructive atelectasis (long arrows) with a higher signal intensity than the central tumor (short arrows). The ability to perform multiplanar imaging and needle insertion at any angle facilitated the selection of an optimal puncture path to reduce the risk of pneumothorax **(B)**. The biopsy specimen revealed squamous cell carcinoma.

separation, 5 mm/1 mm; field of view, 350 mm × 299 mm; matrix, 220 x 176; NSA, 2; and acquisition time, 1 minute 3 seconds) was employed to check for pneumothorax; and chest radiography or CT was performed 24 hours later. If a small asymptomatic pneumothorax was present, conservative treatment was administered with monitoring of vital signs and administration of supplemental oxygen. If a large (lung surface retraction ≥30%) or rapidly expanding pneumothorax developed, a pleural drain was inserted. Pneumothorax, pleural drainage, hemoptysis, and other possible complications were recorded.

Data Analysis

Technical success was defined as the acquisition of a tissue specimen adequate for pathological analysis. The specific histological types of the samples were recorded. Final diagnoses were determined by surgical confirmation or clinical follow-up results for at least 24 months. A final diagnosis of negative for malignancy was made when any of the following conditions were met: 1) no malignant tumor was identified during surgery, 2) spontaneous regression of the lesion occurred, 3) no lesion growth was found on subsequent follow-up imaging for more than 24 months, and 4) resolution of the lesion occurred after treatment for conditions other than cancer.

The diagnostic accuracy, sensitivity, specificity, positive predictive value, and negative predictive value of percutaneous biopsy for diagnosing lung malignancies were calculated by comparison with the final diagnoses. Complications were classified as minor or major according to the Society of Interventional Radiology Clinical Practice Guidelines' criteria.

RESULTS

Patient Characteristics

The characteristics of the study patients and lung lesions are summarized in Table 2. One hundred and two patients underwent contrast-enhanced CT within 2 weeks before the biopsy procedure, and five patients underwent non-contrast CT due to iodine contrast media allergy (three cases) or renal insufficiency (two cases). The central lesions could be distinguished from post-obstructive atelectasis with CT in 62 patients, but were difficult to distinguish in 45 patients. In 33 and 16 patients, respectively, bronchoscopy- and CT-guided biopsies had previously failed to yield adequate samples or provided indeterminate results. The remaining patients had not undergone lung biopsy by bronchoscopy or CT. All patients were hospitalized.

MRI Findings

In the 107 patients, 96 (89.7%) could be clearly distinguished from post-obstructive atelectasis by multiparameter MRI (central lesion diameter, 1.9–5.6 cm;

https://doi.org/10.3348/kjr.2024.0818

Korean Journal of Radiology
KJR

Table 2. Characteristics of patients and lung lesions (n = 107)

Characteristics	Data
Age, yrs	57.1 ± 10.7
Sex	
Male	68 (63.6)
Female	39 (36.4)
Location of the lung lesions	
Right lower lobe	13 (12.1)
Right middle lobe	17 (15.9)
Right upper lobe	20 (18.7)
Left lower lobe	23 (21.5)
Left upper lobe	34 (31.8)
Prior investigations to obtain diagnosis	
Bronchoscopy	33 (30.8)
CT-guided biopsy	16 (15.0)
None	58 (54.2)
Distinguishing ability on CT	
Typical imaging features	62 (57.9)
No typical imaging features	45 (42.1)

Data are presented as mean ± standard deviation or n (%).

mean diameter, 3.1 ± 1.0 cm). In 89 cases, lesions were distinguished from atelectasis using fast T2WI-TSE and enhanced fast T1WI-TSE, and the distinction could be performed using only fast T2WI-TSE in 72 patients. The remaining seven cases required DWI. Forty-one patients had central lesions with post-obstructive atelectasis in the entire lobe, and 55 had lesions with segmental or local post-obstructive atelectasis. No typical MR findings of central lesions with atelectasis were observed in the other 11 patients (whole-lesion diameter, 6.7–11.3 cm; mean diameter, 8.2 ± 1.3 cm) (Fig. 5).

MRI-Guided Biopsy Results

One hundred and seven suspicious central lung lesions with associated post-obstructive atelectasis in 107 patients were biopsied using MR-guided percutaneous coaxial cutting biopsy. The procedural characteristics are summarized in Table 3. All patients tolerated the MRI-guided percutaneous biopsy procedure well. Adequate specimens for diagnosis were obtained from all the patients, with a technical

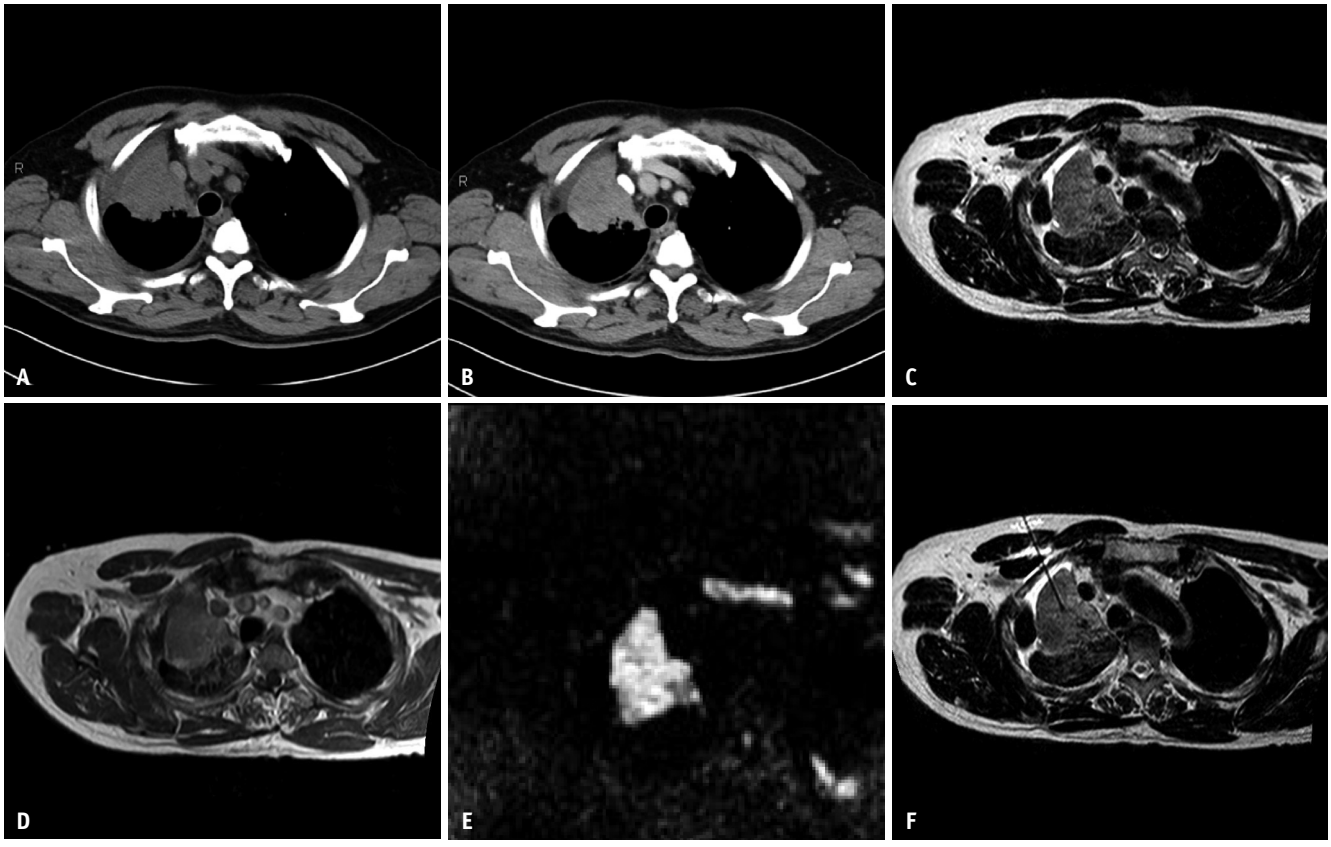

Fig. 5. A 66-year-old male with a lesion in the right upper lobe. The bronchoscopy results were negative. **A, B:** Non-contrast CT **(A)** and enhanced CT **(B)** show suspicious central lesions with atelectasis. **C-E:** However, no typical imaging features are observable on fast T2-weighted imaging-turbo spin echo **(C)**, enhanced fast T1-weighted imaging **(D)**, and diffusion-weighted imaging **(E)**. **F:** Multiplanar MRI-guided puncture of the lesion. The biopsy specimen revealed an adenocarcinoma.

https://doi.org/10.3348/kjr.2024.0818

Table 3. Procedural characteristics of MRI-guided percutaneous biopsy

Characteristics	Data
Distance, cm	
From skin to parietal pleura	8.5 ± 1.3 (6.5–11.0)
From skin to lesion	3.4 ± 0.8 (2.1–5.0)
Lesion diameter, cm	
Typical imaging features on MRI	3.1 ± 1.0 (1.9–5.6)
No typical imaging features on MRI	8.2 ± 1.3 (6.7–11.3)
Cutting needle	
18G	63 (58.9)
20G	44 (41.1)
The number of cores obtained	
3–5	66 (61.7)
6–7	41 (38.3)
Procedural time, min	36.7 ± 8.7 (27.0–67.0)
Complications	
None	99 (92.5)
Pneumothorax	5 (4.7)
Self-limited hemoptysis	3 (2.8)

Data are presented as mean ± standard deviation (range) or n (%)

Table 4. Characterization of specific type of percutaneous biopsy and final diagnoses

Lesions	Percutaneous biopsy	Final diagnoses
Malignant	98	101
Adenocarcinoma	45	46
Squamous cell carcinoma	35	37
Small cell carcinoma	14	14
Poorly differentiated cancer	3	3
Atypical carcinoid	1	1
Benign	9	6
Fibrous tissue	4	3
Chronic inflammation	3	2
Pulmonary tuberculosis	1	1
Chronic inflammation with atypical hyperplasia of alveolar epithelium	1	0

success rate of 100%. The biopsy procedure time, which was defined as the interval from pre-procedural MRI until needle removal, varied from 27 to 67 minutes (mean, 36.7 ± 8.7 minutes). Of the 107 lesions, 98 were malignant and nine were benign on MRI-guided biopsy. Finally, 101 malignant and six benign lesions were confirmed on the basis of surgical histopathological results (n = 25) or clinical follow-up findings (n = 82). Among the 49 patients who had previously received negative results for malignancy from bronchoscopic biopsy or CT-guided percutaneous biopsy, 47 showed positive results in MRI-guided percutaneous biopsy.

Among the 101 malignant lesions, 98 were diagnosed as true-positive and three as false-negative by percutaneous MRI-guided biopsy (Table 4). The first false-negative case was diagnosed as proliferative fibrous tissue by percutaneous biopsy; however, surgical resection was performed, and the histopathological diagnosis was squamous cell carcinoma. In the second case, chronic pulmonary inflammation with atypical hyperplasia of the alveolar epithelium was diagnosed using percutaneous biopsy, and EBUS-TBNA after three months confirmed squamous cell carcinoma. The third patient was diagnosed as showing pulmonary fibrosis with chronic inflammation by percutaneous biopsy; however, subsequent surgical histopathology confirmed an adenocarcinoma. Among the other six patients in this study who received a negative diagnosis through MRI-guided biopsy, one patient with pulmonary tuberculosis was cured after anti-tuberculosis therapy, two patients with chronic inflammation showed significant improvement after anti-infection treatment, and three patients with fibrous tissue exhibited no remarkable changes during a follow-up period of over 24 months.

The sensitivity, specificity, positive predictive value, negative predictive value, and accuracy of MRI-guided percutaneous biopsy for diagnosing lung malignancy were 97.0% (98/101), 100% (6/6), 100% (98/98), 66.7% (6/9), and 97.2% (104/107), respectively. Self-limiting hemoptysis occurred in three patients (2.8%, 3/107). Pneumothorax occurred in five patients (4.7%, 5/107), of which none required pleural drainage. No serious procedure-related complications occurred.

DISCUSSION

Because biopsy provides only small tumor fragments, the most suspicious areas should be identified to obtain sufficient tumor-representative materials for analysis [16]. In this study, multiparameter MRI was used as a guidance method to distinguish between tumors and atelectasis in most cases. MRI-guided percutaneous biopsy for diagnosing lung malignancy showed an accuracy of 97.2% for suspicious centrally located lung lesions with associated post-obstructive atelectasis, and no serious procedure-related complications were observed.

Although evaluation of the lungs by MRI is limited by the low proton density of normal lung tissue, respiratory motion, and cardiovascular pulsation artifacts, MRI provides

https://doi.org/10.3348/kjr.2024.0818

Korean Journal of Radiology
KJR

unparalleled soft-tissue contrast, multiparameter imaging, and functional imaging to reflect tissue heterogeneity [11,14,17,18]. On T2WI, atelectasis and post-obstructive pneumonia often exhibit higher signal intensities than the central tumor. Previous studies have reported that approximately 70%–80% of cases can be identified on T2WI [1,2,19,20]. In contrast, atelectasis is characterized by lung collapse. In comparison with normal lung parenchyma, atelectasis tissue shows more blood vessels per volume than normal lung tissue. Therefore, atelectasis usually shows a higher signal intensity than the central tumor on contrast-enhanced T1WI, which may help distinguish obstructive atelectasis from lesions. In this study, fast T2WI-TSE and enhanced fast T1WI-TSE sequences were preferentially used to locate lesions, and these sequences could successfully distinguish atelectasis in 89 patients; in 72 patients, atelectasis was distinguishable using only fast T2WI-TSE. If these two sequences could not conclusively distinguish lesions and atelectasis, DWI was used for supplementary scanning. Previous reports have shown that DWI is feasible for distinguishing lung cancer from post-obstructive lung collapse, and that pre-procedural DWI is helpful in identifying biopsy targets [2,21,22-24]. In our study, DWI facilitated the diagnosis of seven additional lesions that could not be determined using T2WI-TSE and enhanced T1WI-TSE. In addition, the ability to arbitrarily choose the imaging plane in MRI is very important for successful location of lesions and for clearly and intuitively displaying lesions with atelectasis in coronal or sagittal images. This study achieved high diagnostic accuracy, which is closely related to the precise determination of the tumor location by multiparameter MRI, and effectively avoided the interference of atelectasis on the puncture target.

CT is the preferred imaging modality for percutaneous lung biopsy. Previous studies have shown that dynamic enhanced CT scans can distinguish between central pulmonary tumors and atelectasis in 80% of the cases [25]. However, in one study, lung cancer and atelectasis were identified in only 42% of cases using bolus-enhanced CT [2]. Moreover, CT-guided percutaneous biopsies are usually performed under non-enhanced scanning conditions. Even enhanced scanning can only provide a transient differentiation effect. When CT fails to distinguish between atelectasis and tumors, performing PET/CT and MRI before CT-guided biopsy may be beneficial. However, identifying the target during CT-guided biopsy based on preoperative PET/CT or MR results is clearly less accurate than continuously determining the relationship between the puncture needle and the target during MRI-guided biopsy.

In comparison with CT and ultrasound, MRI is time-consuming when performing percutaneous biopsies. The long procedure time limits the usability of MRI guidance for procedures involving aged patients and those with a poor constitution, especially when local anesthesia is used. In our study, the procedure time was relatively short, ranging from 27 to 67 minutes (mean, 36.7 ± 8.7 minutes). Several measures were employed to shorten the procedure time. First, a fast scan sequence (fast T2WI-TSE: 39 seconds; fast T1WI-TSE: 40.3 seconds) was used to replace the conventional diagnostic sequence (conventional T2WI-TSE: 3 minutes; conventional T1WI-TSE: 2 minutes 58 seconds), which reduced the acquisition time while ensuring sufficient imaging quality. Second, although DWI has been reported to be of great value in distinguishing tumors from atelectasis, it can be time-consuming (2 minutes 54 seconds) and is susceptible to artifacts caused by chemical shifts, phase-encoding direction, the puncture needle, and respiratory and cardiac motions [20]. Thus, its use should usually be considered for partial lesions that cannot be clearly distinguished on fast conventional sequences. Consequently, it was not routinely used for all patients in our study. Finally, because MR pulmonary imaging is susceptible to respiratory motion artifacts, respiratory gating is often used to facilitate image acquisition, especially in the lower lungs [15]. However, this significantly extends the procedural time. Therefore, we only used respiratory gating to locate the lesion before the procedure and to determine the final position of the puncture needle, rather than actual guidance. This reduced the time required for respiratory gating.

Because the central lesion is adjacent to the hilum, avoidance of vascular injury during the procedure is the key to safety. The flowing void effect of MRI clearly shows the relationship between the lesion and pulmonary vessels without the need for a contrast agent; thus, the operator can avoid puncturing the vessels during the procedure, reducing the risk of vascular injury. In this study, only three patients experienced self-limiting hemoptysis, and no serious bleeding complications occurred. In addition, MRI can be advantageous for evaluating patients with adverse reactions to intravenous contrast or impaired renal function [14]. Pneumothorax is the most common complication of percutaneous lung biopsy [26]. The incidence of pneumothorax was low in the present study (4.7%). The puncture approach was optimized to pass

 https://doi.org/10.3348/kjr.2024.0818

through the atelectasis tissue as much as possible to avoid pneumothorax. If the puncture passed through normal lung parenchyma, normal saline was injected into the needle passage to seal the needle passage. The literature indicates that sealing the puncture access with saline can significantly reduce the incidence of pneumothorax and prevent subsequent chest tube placement after percutaneous lung biopsy [27,28].

Our study had three important limitations. First, "gold standard" surgical pathology was performed after percutaneous biopsy in only a small number of patients (25 patients) since most patients had advanced lung cancer, small cell cancer, or advanced age. Second, we did not perform direct comparisons with CT- or bronchoscopy-guided biopsy. Third, the low proportion of patients with pneumothorax in this study may be related to the fact that not all cases were confirmed on CT.

In conclusion, multiparameter MRI allowed distinction of central lung tumors from atelectasis and facilitated accurate and safe guided percutaneous biopsy. MRI-guided percutaneous biopsy may be of value in the diagnosis of central lung disease with associated atelectasis, especially when contrast-enhanced CT yields unclear results and when bronchoscopy fails or shows negative results. Future studies should aim to compare MRI-guided percutaneous biopsy with CT-guided percutaneous biopsy and bronchoscopic biopsy.

Availability of Data and Material

The datasets generated or analyzed during the study are not publicly available regarding personal privacy, but are available from the corresponding author on reasonable request.

Conflicts of Interest

The authors have no potential conflicts of interest to disclose.

Author Contributions

Conceptualization: all authors. Data curation: all authors. Formal analysis: Peipei Li, Chengli Li, Yujun Xu. Investigation: all authors. Methodology: Peipei Li, Xiangmeng He, Chengli Li, Ming Liu. Resources: all authors. Writing—original draft: Peipei Li. Writing—review & editing & revise: Ming Liu, Chengli Li.

ORCID IDs

Peipei Li
https://orcid.org/0009-0008-9664-9256
Chengli Li
https://orcid.org/0009-0001-6579-6332
Yujun Xu
https://orcid.org/0009-0007-2579-3720
Xiangmeng He
https://orcid.org/0000-0003-1942-8181
Roberto Blanco Sequeiros
https://orcid.org/0000-0002-0167-9639
Ming Liu
https://orcid.org/0009-0001-3552-6139

Funding Statement

This research has been supported by Natural Science Foundation of Shandong Province (ZR2020MH228).

Acknowledgments

We would like to thank all participants for their support in this study.

REFERENCES

1. Bourgouin PM, McLoud TC, Fitzgibbon JF, Mark EJ, Shepard JA, Moore EM, et al. Differentiation of bronchogenic carcinoma from postobstructive pneumonitis by magnetic resonance imaging: histopathologic correlation. *J Thorac Imaging* 1991;6:22-27
2. Qi LP, Zhang XP, Tang L, Li J, Sun YS, Zhu GY. Using diffusion-weighted MR imaging for tumor detection in the collapsed lung: a preliminary study. *Eur Radiol* 2009;19:333-341
3. Tournoy KG, Rintoul RC, van Meerbeeck JP, Carroll NR, Praet M, Buttery RC, et al. EBUS-TBNA for the diagnosis of central parenchymal lung lesions not visible at routine bronchoscopy. *Lung Cancer* 2009;63:45-49
4. Hagmeyer L, Fassunke J, Engels M, Treml M, Herkenrath S, Matthes S, et al. Bronchoscopic brushing from central lung cancer-next generation sequencing results are reliable. *Lung* 2019;197:333-337
5. Verma A, Jeon K, Koh WJ, Suh GY, Chung MP, Kim H, et al. Endobronchial ultrasound-guided transbronchial needle aspiration for the diagnosis of central lung parenchymal lesions. *Yonsei Med J* 2013;54:672-678
6. Tang CL, Zhu Z, Zhong CH, Zhou ZQ, Zhou HQ, Geng RM, et al. Clinical application of endobronchial ultrasonography-guided transbronchial needle aspiration biopsy-a single center, large sample, real-world study. *BMC Pulm Med* 2023;23:336
7. Zhu J, Liu R, Wu X, Li Q, Gong B, Shen Y, et al. The value of narrow-band imaging bronchoscopy in diagnosing central lung cancer. *Front Oncol* 2022;12:998770
8. Sagar AS, Sabath BF, Eapen GA, Song J, Marcoux M, Sarkiss M, et al. Incidence and location of atelectasis developed during bronchoscopy under general anesthesia: the I-LOCATE trial.

Chest 2020;158:2658-2666
9. Ghossein J, Gingras S, Zeng W. Differentiating primary from secondary lung cancer with FDG PET/CT and extra-pulmonary tumor grade. *J Med Imaging Radiat Sci* 2023;54:451-456
10. Zukotynski KA, Gerbaudo VH. Understanding the value of FAPI versus FDG PET/CT in primary and metastatic lung cancer. *Radiology* 2023;308:e231768
11. Abrishami Kashani M, Campbell-Washburn AE, Murphy MC, Catalano OA, McDermott S, Fintelmann FJ. Magnetic resonance imaging for guidance and follow-up of thoracic needle biopsies and thermal ablations. *J Thorac Imaging* 2022;37:201-216
12. Ohno Y, Ozawa Y, Nagata H, Ueda T, Yoshikawa T, Takenaka D, et al. Lung magnetic resonance imaging: technical advancements and clinical applications. *Invest Radiol* 2024;59:38-52
13. Ohno Y, Ozawa Y, Koyama H, Yoshikawa T, Takenaka D, Nagata H, et al. State of the art MR imaging for lung cancer TNM stage evaluation. *Cancers (Basel)* 2023;15:950
14. Barreto MM, Rafful PP, Rodrigues RS, Zanetti G, Hochhegger B, Souza AS Jr, et al. Correlation between computed tomographic and magnetic resonance imaging findings of parenchymal lung diseases. *Eur J Radiol* 2013;82:e492-e501
15. Liu M, Huang J, Xu Y, He X, Li L, Lü Y, et al. MR-guided percutaneous biopsy of solitary pulmonary lesions using a 1.0-T open high-field MRI scanner with respiratory gating. *Eur Radiol* 2017;27:1459-1466
16. Guimaraes MD, de Andrade MQ, da Fonte AC, Chojniak R, Gross JL. CT-guided cutting needle biopsy of lung lesions--an effective procedure for adequate material and specific diagnose. *Eur J Radiol* 2011;80:e488-e490
17. Owens C, Hindocha S, Lee R, Millard T, Sharma B. The lung cancers: staging and response, CT, 18F-FDG PET/CT, MRI, DWI: review and new perspectives. *Br J Radiol* 2023;96:20220339
18. Tang X, Bai G, Wang H, Guo F, Yin H. Elaboration of multiparametric MRI-based radiomics signature for the preoperative quantitative identification of the histological grade in patients with non-small-cell lung cancer. *J Magn Reson Imaging* 2022;56:579-589
19. Tobler J, Levitt RG, Glazer HS, Moran J, Crouch E, Evens RG. Differentiation of proximal bronchogenic carcinoma from postobstructive lobar collapse by magnetic resonance imaging. Comparison with computed tomography. *Invest Radiol* 1987;22:538-543
20. Yang RM, Li L, Wei XH, Guo YM, Huang YH, Lai LS, et al. Differentiation of central lung cancer from atelectasis: comparison of diffusion-weighted MRI with PET/CT. *PLoS One* 2013;8:e60279
21. Horn M, Oechsner M, Gardarsdottir M, Köstler H, Müller MF. Dynamic contrast-enhanced MR imaging for differentiation of rounded atelectasis from neoplasm. *J Magn Reson Imaging* 2010;31:1364-1370
22. Guimaraes MD, Marchiori E, Odisio BC, Hochhegger B, Bitencourt AG, Zurstrassen CE, et al. Functional imaging with diffusion-weighted MRI for lung biopsy planning: initial experience. *World J Surg Oncol* 2014;12:203
23. Matoba M, Tonami H, Kondou T, Yokota H, Higashi K, Toga H, et al. Lung carcinoma: diffusion-weighted MR imaging--preliminary evaluation with apparent diffusion coefficient. *Radiology* 2007;243:570-577
24. Guimarães MD, Hochhegger B, Benveniste MF, Odisio BC, Gross JL, Zurstrassen CE, et al. Improving CT-guided transthoracic biopsy of mediastinal lesions by diffusion-weighted magnetic resonance imaging. *Clinics (Sao Paulo)* 2014;69:787-791
25. Onitsuka H, Tsukuda M, Araki A, Murakami J, Torii Y, Masuda K. Differentiation of central lung tumor from postobstructive lobar collapse by rapid sequence computed tomography. *J Thorac Imaging* 1991;6:28-31
26. Avritscher R, Krishnamurthy S, Ensor J, Gupta S, Tam A, Madoff DC, et al. Accuracy and sensitivity of computed tomography-guided percutaneous needle biopsy of pulmonary hilar lymph nodes. *Cancer* 2010;116:1974-1980
27. Li Y, Du Y, Luo TY, Yang HF, Yu JH, Xu XX, et al. Usefulness of normal saline for sealing the needle track after CT-guided lung biopsy. *Clin Radiol* 2015;70:1192-1197
28. Billich C, Muche R, Brenner G, Schmidt SA, Krüger S, Brambs HJ, et al. CT-guided lung biopsy: incidence of pneumothorax after instillation of NaCl into the biopsy track. *Eur Radiol* 2008;18:1146-1152

 https://doi.org/10.3348/kjr.2024.0818